PHYSICAL REVIEW C **73**, 014610 (2006)

Charge density distributions and charge form factors of the $N = 82$ and $N = 126$ isotonic nuclei

Zaijun Wang,[1,*] Zhongzhou Ren,[1,2,†] and Ying Fan[1]

[1]*Department of Physics, Nanjing University, Nanjing 210008, China*

[2]*Center of Theoretical Nuclear Physics, National Laboratory of Heavy-Ion Accelerator at Lanzhou, Lanzhou 730000, China*

(Received 27 June 2005; published 26 January 2006)

Charge form factors for $N = 82$ and $N = 126$ isotonic nuclei are calculated with the relativistic eikonal approximation, in which the charge density distributions are from the relativistic mean-field theory. The variations of charge form factors with proton number are discussed in detail. It is found that the most sensitive parts of the charge form factors are those around the minimums and maximums. For an increasing proton number, the charge form factors near the extrema have an upward shift. As the protons increase and occupy a new shell, the minimums and maximums of the charge form factors could also have a significant inward shift. The results can be useful for the study of behaviors of valence-proton wave functions for such nuclei as can be considered as a core plus proton(s), and thus the proton-halo phenomenon. In addition, the results can also be useful for future electron-unstable nucleus scattering experiments and provide tests of the reliability of the relativistic mean-field theory for the unstable nuclei.

DOI: 10.1103/PhysRevC.73.014610 PACS number(s): 25.30.Bf, 21.10.Ft, 13.40.Gp

I. INTRODUCTION

Most of our knowledge of nuclear physics is obtained from the study of stable nuclei on and near the stability line. Recently, the development of radioactive-isotope- (RI-) beam techniques [1–3] has opened a new field for the study of unstable nuclei far from the stability line. As a result, our knowledge of nuclear physics has also been extended from stable nuclei to unstable ones. Experiments with RI beams [4–16] have already shown that the properties of unstable nuclei are quite different from those of stable ones [17–32]. Therefore it is very interesting to investigate the properties of unstable nuclei theoretically with reliable theories or models. The results will provide references for future experiments as well as tests of reliability of the well-established nuclear theory for unstable nuclei.

Nuclear charge density distribution is one of the basic quantities to describe the nuclear properties. The charge densities can give us much detailed information on the internal structure of nuclei since they are directly related to the wave functions of protons, which are of key importance for many calculations in nuclear physics. Electron-nucleus scattering is known to be one of the powerful tools for investigating nuclear charge density distributions. Charge density distributions for stable nuclei have been well studied with this method [33–38]. For unstable nuclei, although studies of electron scattering have not been realized so far, nuclear physicists have already planned to explore the structures of unstable nuclei with electron-nucleus scattering. Based on the new techniques for producing high-quality RI beams, new electron-nucleus colliders are now under construction at RIKEN in Japan [39,40] and at GSI in Germany [41,42]. One of the main subjects of the new colliders is the measurement of charge form factors for unstable nuclei. Therefore it is expected that information on the charge density distributions of unstable nuclei will soon be available.

In parallel with the experimental projects, it is then clear that theoretical studies on electron scattering from unstable nuclei also need to be made. We note that some research on this topic has already been made. To find out if the charge distributions for unstable nuclei can be measured by electron–RI-beam scattering, T. Suda [40] studied the sensitivity of the charge form factor to a change of charge distribution in terms of the two-parameter Fermi model. He found that both the minimums and maximums of the charge form factors were very sensitive to a change in the size and diffuseness parameters. Some other important studies on this topic have also been made by Moya de Guerra *et al.* [43] with charge densities from nonrelativistic Hartree-Fock calculations with Skyrme forces and by A. N. Antonov *et al.* [44,45] with phenomenological charge densities. In addition, we have also made contributions to this aspect. We investigated the sensitivity of charge form factors to the extended charge distributions of light exotic proton-rich nuclei [46] and the variations of the charge form factors with neutron number for medium-heavy and heavy isotopic chains [47] in the relativistic frame by using the relativistic eikonal approximation (REA) associated with the relativistic mean-field (RMF) model. These studies have shown that the isotopic shifts of the charge form factor, i.e., the effect of different neutron numbers on the proton density distribution, can be measured by the electron–RI-beam experiments. Studies of charge form factors on isotopic chains can reveal the effect of neutrons on the distribution of protons. This effect is especially important for the unstable nuclei in the neutron-rich region. Therefore this research is of course very important to our understanding of nuclear properties, whereas if we want to know the details of wave function of a certain shell or shells, it would be better to explore the variation of charge form factors with the proton number along isotonic chains. This is because the proton density distributions are a sum of the proton wave functions squared. Therefore the difference of the charge density distributions of two isotonic nuclei will certainly reveal the behavior of the proton wave functions of a certain shell. Thus it would be of great interest to

*Electronic address: zaijunwang99@hotmail.com

†Electronic address: zren@nju.edu.cn

make theoretical and experimental studies on elastic electron scattering from isotonic nuclei. In addition, we have found few calculations and discussions of electron scattering along isotonic chains so far. Therefore, in this paper, we attempt to calculate the charge form factors for some specially chosen isotonic chains and analyze the variations of charge form factors with the proton number. The $N = 82$ and $N = 126$ isotonic chains are two appropriate isotonic chains. First, the neutron numbers are magic numbers. Second, on these two isotonic chains, there are stable nuclei as well as unstable ones. The isotones ^{136}Xe, ^{138}Ba, ^{140}Ce, and ^{144}Sm on the $N = 82$ chain and ^{206}Hg, ^{208}Pb on the $N = 126$ chain are stable nuclei, and, in particular, ^{138}Ba and ^{140}Ce are highly abundant in nature. Therefore the electron-scattering experiment on these stable isotones can be easily carried out under the present experimental conditions, and the results can be used as references for the possible electron-nucleus colliding experiment on the other unstable isotones on these two isotonic chains. In addition, although ^{210}Po on the $N = 126$ chain is an unstable nucleus, it has a very long half-life, $T_{1/2} = 138$ days and it can be produced from the natural α-decay chain starting from ^{238}U. Therefore it is possible to do an electron-scattering experiment on ^{210}Po with the help of natural radioactivity. Thus, from this point of view, theoretical investigations on these two isotonic chains will be very interesting.

In our previous papers, [46,47], we successfully combined the REA with the RMF model for elastic electron-nucleus scattering. We systematically tested this method (REA+RMF) for nuclei in the light-mass region [46,47]. For the medium-heavy and heavy regions, we tested this method with ^{40}Ca, ^{58}Ni, and ^{208}Pb. It has been found that the method is very stable and reliable. To ensure the reliability of the calculations in this paper, we further tested it with ^{126}Sn and ^{208}Pb for the TM1 parameter set, which is used in the present work. We calculated the cross sections for ^{124}Sn (we plotted the cross sections and absolute values of the form factors and compared them with Fig. 1 of Ref. [48] and Fig. 1 of Ref. [49]; the results are not given here) and ^{208}Pb (see Fig. 6 in the next section; the filled circles are experimental cross sections and the dashed curves are the calculated ones, and the plots are multiplied by 100 for clarity) and compared the results with the experimental ones [48–50]. It was found that the calculated cross sections were in good agreement with the experimental ones. Therefore, in this paper, we further use this method to calculate the charge form factors for the above-mentioned isotonic chains and analyze the variations of the charge form factors with the proton number. It is expected that the results can be useful for possible future experiments and will also provide new tests of the RMF theory for the unstable nuclei.

II. CALCULATIONS AND DISCUSSIONS

To begin, we give a short review of the method developed in Refs. [46,47,51]. The REA method is for the high-energy electron scattering. From the Dirac equation for a particle moving in a scalar potential $V(\mathbf{r})$,

$$(\alpha \cdot \mathbf{p} + \beta m - E)\psi(\mathbf{r}) = -V(\mathbf{r})\psi(\mathbf{r}), \tag{1}$$

the elastic differential cross section σ for a charged particle can be derived [51]:

$$\sigma = \cos^2\left(\frac{1}{2}\theta\right) | -ik \int_0^R J_0(qb)[e^{2i\chi(b)} - 1]b\,db - ik \times \int_R^\infty J_0(qb)[e^{2i\chi(b)} - 1]b\,db|^2, \tag{2}$$

where E and m are the energy and mass of the incident particles, respectively; α and β are the Dirac matrices; θ is the scattering angle; and J_0 is the Bessel function. $\chi(b)$ is the phase-shift function that can be expressed as

$$\chi(b) = \begin{cases} -\alpha Z \ln\left(\frac{b}{R}\right), & b > R \\ -Z\alpha \log\left(\frac{b}{R}\right) - 4\pi\alpha \int_b^R r^2\rho(r)y(\frac{b}{r})\,dr, & b < R \end{cases}, \tag{3}$$

where b is the impact parameter and R is the cutoff radius of the charge density distribution.

From Eq. (3), it is clear that the differential cross sections are directly related to the nuclear charge density distribution. In this work, the nuclear charge density distributions are generated by use of the reliable and widely used RMF model. After the differential cross sections are obtained, we can calculate the charge form factors $F(q)$ by dividing the differential cross sections with the Mott cross section σ_M:

$$|F(q)|^2 = \frac{\sigma}{\sigma_M}, \tag{4}$$

where

$$\sigma_M = \frac{\alpha^2(\hbar c)^2 \cos^2\frac{\theta}{2}}{4E^2 \sin^4\frac{\theta}{2}}. \tag{5}$$

Since we are dealing with high-energy electron scattering off heavy nuclei, the Coulomb attraction felt by the electrons must be taken into account. We do this with the standard method in electron scattering, that is, we replace the momentum transfer q with the effective momentum transfer,

$$q_{\mathrm{eff}} = q\left(1 + \frac{3}{2}\frac{Z\hbar c}{ER_0}\right), \tag{6}$$

in our calculation, where $R_0 = 1.07\,A^{1/3}$ and A is the mass number of the nucleus.

The RMF model originally developed from the pioneering work by Walecka [52,53] and now has become the standard theory in describing nuclear matter and nuclear properties. Recently, this model has been extensively used to describe the properties of the ground and the low excited states for both stable nuclei and for unstable ones. Detailed reviews have been given by Serot and Walecka [54]. The details for the RMF model can also be found in many other articles such as [55–62]. We do not discuss them here.

With the method described above, we can calculate the cross sections and charge form factors for the $N = 82$ and $N = 126$ isotonic chains. In the calculation of the charge form factors, we obtain the charge densities here by folding the point proton densities with the proton charge density distribution [63]:

$$\rho_p(r) = \frac{Q^3}{8\pi}e^{-Qr}, \tag{7}$$

TABLE I. The RMF results with the TM1 parameter set and the corresponding experimental values for the $N = 82$ isotonic nuclei.

Nuclide	Z	E/A (MeV)	E/A(expt) (MeV)	R (fm)	R(expt) (fm)
^{132}Sn	50	8.343	8.355	4.739	
^{134}Te	52	8.389	8.383	4.783	
^{136}Xe	54	8.416	8.396	4.824	4.800
^{138}Ba	56	8.434	8.393	4.862	4.839
^{140}Ce	58	8.434	8.376	4.899	4.880
^{144}Sm	62	8.338	8.303	4.965	4.976
^{146}Gd	64	8.270	8.250	4.996	
^{148}Dy	66	8.164	8.181	5.037	

where $Q^2 = 18.29\,\mathrm{fm}^2 = 0.71\,\mathrm{GeV}^2(\hbar c = 0.197\,\mathrm{GeV\ fm} = 1)$. The corresponding rms charge radius of the proton is $r_p = 0.81$ fm.

We first produce the charge density distributions by using the RMF model. Since we are now dealing with medium-heavy and heavy nuclei, we use the TM1 force parameter set [60], which was put forward especially for heavy nuclei to carry out the RMF calculations. The RMF results are presented in Table I, Table II, and Figs. 1 and 2.

In Tables I and II, we list the theoretical average binding energies, rms charge radii, and the corresponding experimental results [38,64]. For the results of the $N = 82$ isotonic chain listed in Table I, the theoretical average binding energies are, at most, only 0.70% off the experimental ones. The deviation between the calculated rms charge radii and the experimental ones is less than 0.025 fm. For the results of the $N = 126$ isotonic chain in Table II, the deviations between the theoretical average binding energies and the experimental ones are less than 1.02%, and those between the calculated rms charge radii and the experimental ones are less than 0.04 fm. These indicate that the RMF results with the TM1 force parameter set are in good agreement with experiments.

In Figs. 1 and 2, we present the variations of the charge density distributions for the two isotonic chains. From Fig. 1 we note that, for the nuclei ^{132}Sn, ^{134}Te, ^{136}Xe, ^{138}Ba, and ^{140}Ce, the inner parts of the charge density distributions tend to become lower as the proton number increases, while the outer parts of the charge density distributions show a reverse trend. Also, there appear to be two peaks in the charge density distributions, which implies that there are shell structures in

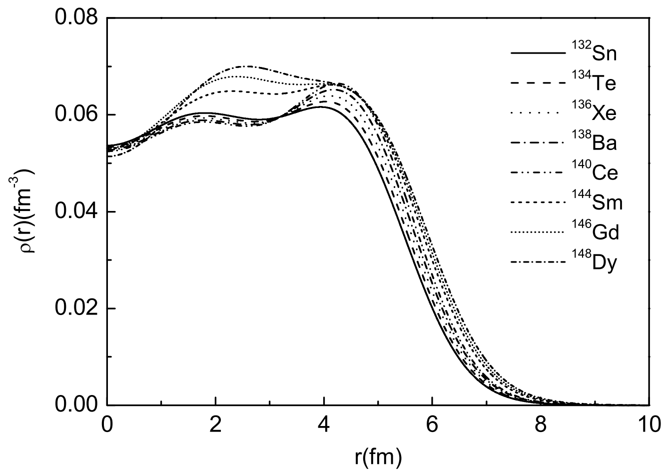

FIG. 1. Variation of charge density distributions for the $N = 82$ isotonic nuclei calculated with the RMF model.

the charge distributions for these nuclei, whereas for ^{144}Sm, ^{146}Gd, and ^{148}Dy the features of the charge distributions are quite different. There is only one peak in the charge distributions. The depression near $r = 3.0$ fm for ^{132}Sn, ^{134}Te, ^{136}Xe, ^{138}Ba, and ^{140}Ce is replaced with this peak. We consider that this peak results mainly from the occupation of the $2d$ shell by the additional protons (relative to ^{140}Ce) as the proton number increases. According to the RMF calculations, including the pairing energy by the Bardeen-Cooper-Schrieffer (BCS) treatment, the level sequence of the subshells in the sixth main shell is $1g_{7/2}, 2d_{5/2}, 1h_{11/2}, 2d_{3/2}, 3s_{1/2}$. Therefore, for ^{144}Sm and ^{146}Gd, the additional protons (relative to ^{140}Ce) mainly occupy the $2d_{5/2}$ level. For ^{148}Dy, the two outermost protons also mainly fill the $1h_{11/2}$ shell. However, according to our calculations, the energy gap between the $1h_{11/2}$ shell and the $2d_{3/2}$ shell is very small, just 0.208 MeV. Thus the two outermost protons of ^{148}Dy can also have quite a large probability on the $2d_{3/2}$ level. Accordingly, we conclude that the additional protons (relative to ^{140}Ce) of ^{144}Sm, ^{146}Gd, and ^{148}Dy are mainly on the $2d$ shell. On the other hand, we plotted

TABLE II. The RMF results with the TM1 parameter set and the corresponding experimental values for the $N = 126$ isotonic nuclei.

Nuclide	Z	E/A (MeV)	E/A(expt) (MeV)	R (fm)	R(expt) (fm)
^{206}Hg	80	7.873	7.869	5.518	
^{208}Pb	82	7.874	7.867	5.543	5.503
^{210}Po	84	7.849	7.834	5.575	
^{212}Rn	86	7.821	7.795	5.606	
^{214}Ra	88	7.790	7.749	5.636	
^{216}Th	90	7.756	7.698	5.666	
^{218}U	92	7.719	7.641	5.695	

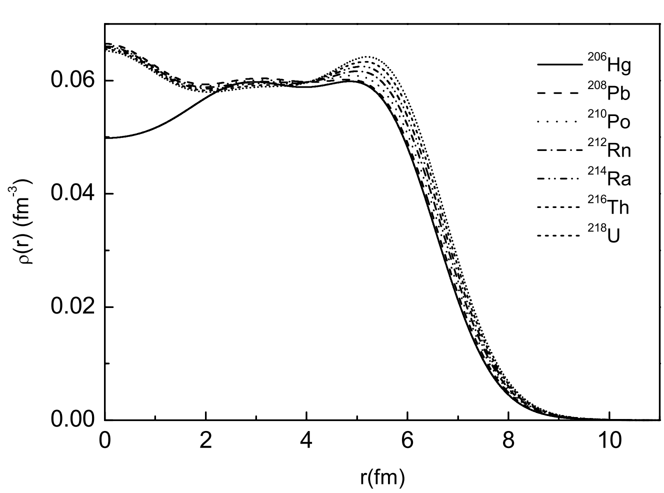

FIG. 2. Variation of charge density distributions for the $N = 126$ isotonic nuclei calculated with the RMF model.

the wave functions squared for the protons on the $2d_{5/2}$ and $2d_{3/2}$ shells. It was found that the wave functions squared peak at $r \approx 3$ fm. Thus it is the occupation of the $2d$ shell and the properties of the wave functions of this shell that have resulted in the peaks around $r = 3.0$ fm in the charge density distributions of ^{144}Sm, ^{146}Gd, and ^{148}Dy.

Figure 2 shows the charge density distributions for the $N = 126$ isotonic nuclei ^{206}Hg, ^{208}Pb, ^{210}Po, ^{212}Rn, ^{216}Th, and ^{218}U. It can be seen that, for the region $r > 4.0$ fm, the charge density distributions tend to become higher and the peak near $r = 6.0$ fm appears more prominent as the proton number increases. For the region $r < 2.50$ fm, there is a great difference in the charge density distributions between ^{206}Hg and the other isotonic nuclei. There is a depression around the origin in the charge density distribution of ^{206}Hg, whereas for the other nuclei, the depression is replaced with a peak. This difference can be accounted for by the shell model. For ^{206}Hg, the last two protons are mainly in the $2d_{3/2}$ state. However, as more protons are added, the $3s_{1/2}$ shell is also occupied and consequently the charge densities around the origin are driven up.

Taking these charge density distributions as inputs, we can further calculate the corresponding charge form factors and cross sections and study their variations with proton number. Figure 3 is the variation of the charge form factors with proton number for the $N = 82$ isotonic chain. In Table III, a more precise quantitative analysis is given of the diffuseness parameters of the charge density distributions, the shifts of minimums, and the form factor differences at $q_{\rm eff} = 1.700$ and 2.302 fm^{-1} for ^{132}Sn, ^{134}Te, ^{136}Xe, ^{138}Ba, and ^{140}Ce. It is seen from Fig. 3 that the curves of the charge form factors can be roughly divided into two groups. One group includes those of ^{132}Sn, ^{134}Te, ^{136}Xe, ^{138}Ba, and ^{140}Ce. The other one consists of ^{144}Sm, ^{146}Gd, and ^{148}Dy. This can also be seen both from the relative shifts listed in the fifth and sixth columns and from the form factor differences listed in the last four columns of Table III, since the shifts and the differences of the charge form factors of ^{144}Sm ^{146}Gd and ^{148}Dy have abrupt increases compared with those of ^{132}Sn, ^{134}Te, ^{136}Xe, ^{138}Ba, and ^{140}Ce. For the first group of nuclei, the charge form factors appear to be almost the same except for an increase in magnitude of the charge form factors near the minimums and maximums. This shows that the shapes of the charge density distributions of these nuclei are not particularly different except near the surface. This agrees with the charge density distributions shown in Fig. 1. The reason is that, although the proton numbers of these nuclei are not the same, their last protons are all mainly in the same shell, i.e., the $1g$ shell. This indicates that, for isotonic nuclei, the shape of the charge density distribution will not be much disturbed when more protons are added to the same shell. For the second group, one can see from Fig. 3 that there is a significant difference in the form factors between these and the first group of nuclei. It is clear from Table III that the shifts of the third and the fourth minimums and the form factor differences both have abrupt increases compared with those of the first group. This inward and upward shift must be from the difference of the charge density distributions between the two groups of nuclei, since the charge form factors are directly related to the charge density distributions. That is, the change of the charge density distributions caused by the occupation of

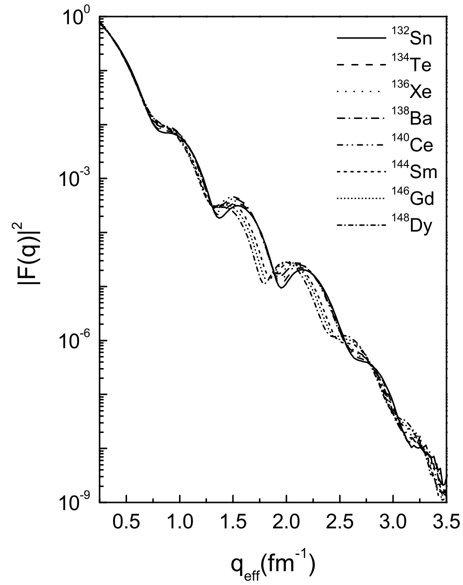

FIG. 3. Variation of the charge form factors with proton number for the $N = 82$ isotonic nuclei ($Z = 50$–66).

TABLE III. The rms radii (R) and diffuseness parameters (a) given by the RMF model. The inward shifts of the second ($\triangle q_{\rm eff1}$), the third ($\triangle q_{\rm eff2}$), and the fourth ($\triangle q_{\rm eff3}$) minimums of the form factors or cross sections relative to those of ^{132}Sn and the form factor differences at $q_{\rm eff} = 1.700$ and 2.302 fm^{-1} predicted by the REA method.

Nuclide	R	a	$\triangle q_{\rm eff1}$	$\triangle q_{\rm eff2}$	$\triangle q_{\rm eff3}$	$q_{\rm eff} = 1.700\,{\rm fm}^{-1}$		$q_{\rm eff} = 2.302\,{\rm fm}^{-1}$	
	(fm)	(fm)	(fm^{-1})	(fm^{-1})	(fm^{-1})	$\|F(q)\|^2$	$\Delta\|F(q)\|^2$	$\|F(q)\|^2$	$\Delta\|F(q)\|^2$
^{132}Sn	4.739	0.468	0.0	0.0	0.0	0.173×10^{-3}	0.0	0.125×10^{-4}	
^{134}Te	4.783	0.465	0.008	0.011	0.013	0.173×10^{-3}	0.000×10^{-3}	0.121×10^{-4}	0.0
^{136}Xe	4.824	0.463	0.026	0.016	0.036	0.172×10^{-3}	0.001×10^{-3}	0.116×10^{-4}	0.005×10^{-4}
^{138}Ba	4.862	0.460	0.050	0.030	0.064	0.170×10^{-3}	0.003×10^{-3}	0.114×10^{-4}	0.007×10^{-4}
^{140}Ce	4.899	0.459	0.055	0.035	0.092	0.168×10^{-3}	0.005×10^{-3}	0.113×10^{-4}	0.008×10^{-4}
^{144}Sm	4.965	0.483	0.064	0.104	0.107	0.702×10^{-4}	0.103×10^{-3}	0.524×10^{-5}	0.069×10^{-4}
^{146}Gd	4.996	0.494	0.069	0.137	0.135	0.440×10^{-4}	0.129×10^{-3}	0.478×10^{-5}	0.073×10^{-4}
^{148}Dy	5.037	0.507	0.069	0.161	0.201	0.230×10^{-4}	0.150×10^{-3}	0.308×10^{-5}	0.090×10^{-4}

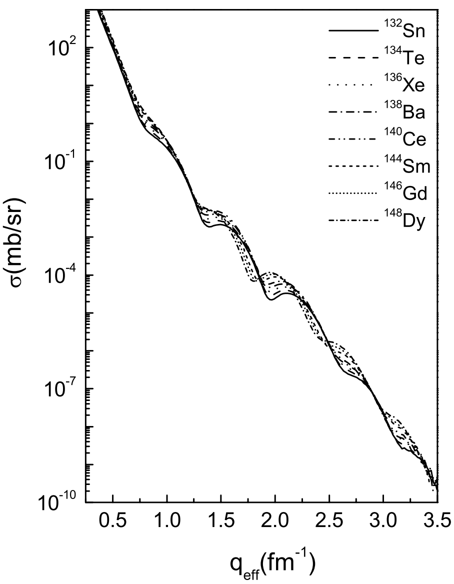

FIG. 4. Variation of the differential cross sections with proton number for the $N = 82$ isotonic nuclei ($Z = 50$–66).

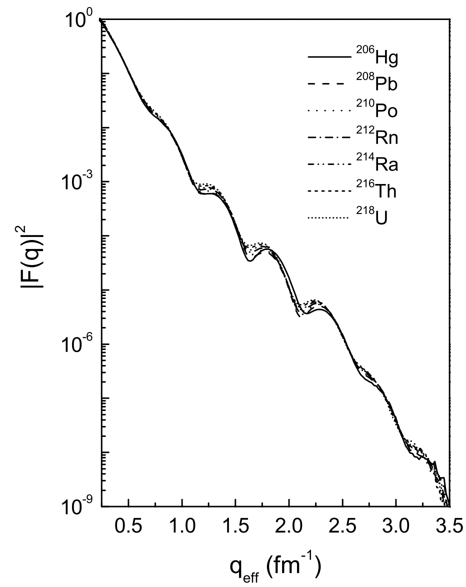

FIG. 5. Variation of the charge form factors with proton number for the $N = 126$ isotonic nuclei ($Z = 80$–92).

the 2d shell is revealed by the inward and upward shift of the charge form factors. The large inward and upward shifts show that the charge form factor is very sensitive to the occupation of a new shell by protons. The largest shifts occur within the range of momentum transfer $1.25\,\text{fm}^{-1} \leqslant q_{\text{eff}} \leqslant 2.75\,\text{fm}^{-1}$. This indicates that the charge form factors within that range of momentum transfer are the most sensitive to a change in proton number. Thus, when the proton number increases and a new shell is occupied, the change of shape of the charge distribution resulting from the occupation of a new proton shell may be observed through electron scattering. Figure 4 is the differential cross sections for these nuclei. One can find that the variational behaviors of the differential cross sections are the same as those of the form factors, and thus the same results and conclusion can be obtained through the analysis of the cross sections.

In Figs. 5 and 6, we show the variation of the charge form factors and cross sections for the $N = 126$ isotonic nuclei. It is seen from Fig. 5 that, different from the $N = 82$ isotonic chain, the charge form factors do not show noticeable inward (or outward) shifts as the proton number changes. The apparent changes of the charge form factors with proton number occur around only the minimums and maximums. This implies that only the charge form factors near the minimums and maximums (or the inflexions) are sensitive to a change in proton number for the heavy isotones. When the proton number increases, the charge form factors near the minimums and maximums both have an increase in magnitude, and the minimums and maximums gradually tend to become inflexions. The quantitative increases in magnitude of the cross sections at $q_{\text{eff}} = 1.660\,\text{fm}^{-1}$ (the position of the third minimum) and $2.190\ \text{fm}^{-1}$ (the position of the fourth minimum) are listed in Table IV, where σ_1 and σ_2 are the magnitudes of the cross sections at $q_{\text{eff}} = 1.660$ and $2.190\ \text{fm}^{-1}$, respectively, and $\triangle\sigma_1$ and $\triangle\sigma_1$ are the magnitude increases relative to those of ^{206}Hg. For instance, the cross section of ^{210}Po at $q_{\text{eff}} = 1.660\,\text{fm}^{-1}$ is 6.363×10^{-4} mb and the increase is 1.773×10^{-4} mb. The increase of the cross section is at least 10 times as large as the experimental errors under the present experimental conditions for stable nuclei [65,66]. This result shows that the charge form factors near the minimums and maximums (or the inflexions) are sensitive to a change in proton number for the heavy isotones; furthermore, the sensitivity may be used to investigate the change of the shape of charge distribution for heavy isotones. There is also another important item to which we should pay attention. As mentioned above, the charge densities near the origin between ^{206}Hg and other isotonic nuclei are quite different (see Fig. 2), whereas from Fig. 5 we cannot find much difference in the charge form

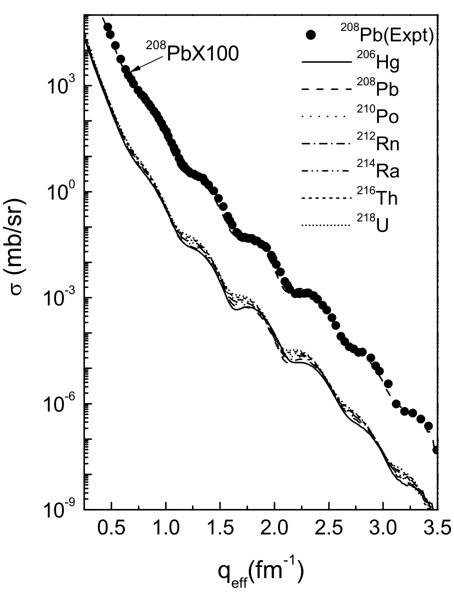

FIG. 6. Variation of the differential cross sections with proton number for the $N = 126$ isotonic nuclei ($Z = 80$–92).

TABLE IV. The rms radii (R), diffuseness parameters (a) given by the RMF model, and the increases of the cross sections at $q_{\mathrm{eff}} = 1.660\ \mathrm{fm}^{-1}$ (the position of the third minimum) and $2.190\ \mathrm{fm}^{-1}$ (the position of the fourth minimum) predicted by the REA method.

Nuclide	R (fm)	a (fm)	σ_1 (mb)	$\Delta\sigma_1$ (mb)	σ_2 (mb)	$\Delta\sigma_2$ (mb)
^{206}Hg	5.518	0.485	4.590×10^{-4}	0.0	1.451×10^{-5}	0.0
^{208}Pb	5.543	0.490	5.392×10^{-4}	0.802×10^{-4}	1.661×10^{-5}	0.210×10^{-5}
^{210}Po	5.575	0.486	6.363×10^{-4}	1.773×10^{-4}	1.960×10^{-5}	0.509×10^{-5}
^{212}Rn	5.606	0.483	7.529×10^{-4}	2.939×10^{-4}	2.272×10^{-5}	0.821×10^{-5}
^{214}Ra	5.636	0.473	8.775×10^{-4}	4.185×10^{-4}	2.608×10^{-5}	1.157×10^{-5}
^{216}Th	5.666	0.465	1.026×10^{-3}	5.607×10^{-4}	2.920×10^{-5}	1.469×10^{-5}
^{218}U	5.695	0.476	1.170×10^{-3}	7.110×10^{-4}	3.309×10^{-5}	1.858×10^{-5}

factors, which indicate the difference in the charge density distributions around the origin. This shows that the charge form factors in the range of momentum transfer considered in this paper are not sensitive to the change of charge densities near the origin. This agrees with the conclusion given in Refs. [65,66]. This also explains why the charge densities extracted from the present electron-nucleus scattering experiments have larger errors near the origin than in the outer part. Therefore we must extend the momentum transfer to a larger value in order to reach more accurate measurements of the charge densities near the origin for the heavy nuclei.

Thus far, we have investigated the variations of the charge form factors with the proton number. It is very interesting to compare the present results with the variations of the charge form factors on isotopic chains. It is known from Refs. [43, 47] that the charge form factors have a significant outward and downward shift as the nucleus moves along the isotopic chains from the neutron-rich region to the neutron-deficient region, whereas for isotonic chains, the charge form factors show an inward and upward shift as the protons increase. The isotopic shifts reveal the effect of the neutrons on the density distributions of the protons, while the isotonic shifts can reflect the influence of the changing proton number on the shape of the proton density distributions. The isotonic shift could be used to investigate the density distribution of the outermost shell protons, and thus the wave functions, of the nuclei. This is especially useful for studies of valence-proton density distributions of such nuclei that can be considered as a core plus one or several protons. For this kind of nuclei, the core is considered to be very weakly disturbed by the valence proton(s), and thus the charge distribution of the core can be considered approximately equal to that of a free nucleus with the same proton and neutron number. Therefore the density distribution of the valence proton(s) could be investigated by a comparison of the charge form factors between the nucleus and its core. In experimental studies, one could determine the valence-proton density distribution by measuring the isotonic shift of the charge form factors. From this point of view, the recently discovered proton-halo phenomenon [24] in the light-mass region may be investigated by a study of the isotonic shift of the charge form factors of the core-plus-proton(s) nuclei.

Finally, it is necessary to analyze to what extent, and under which conditions, future experiments may have the required precision to be sensitive to the shifts predicted in this paper. It is known from Refs. [65,66] that, under the present conditions for stable nuclei, the elastic electron-nucleus scattering experimental data can be taken at intervals as small as 2° of scattering angle. At an incident energy of 500 MeV, this corresponds to a momentum transfer interval of about $0.08\ \mathrm{fm}^{-1}$. The experimental errors of the cross sections at moderate momentum transfers are less than 5.0%. The incident energy can be up to 700 MeV or higher, which has extended the measurements of cross sections to a momentum transfer of about $4\ \mathrm{fm}^{-1}$. Thus, if the nuclei considered in this paper were stable, the shifts of ^{144}Sm, ^{146}Gd, and ^{148}Dy shown in Table III and the increases of the cross sections of ^{208}Pb, ^{210}Po, ^{212}Rn, ^{216}Th, and ^{218}U shown in Table IV could be measured under the present experimental conditions. As a matter of fact, we are now dealing with unstable nuclei. Measurements of electron-scattering cross sections on unstable nuclei will be more difficult. However, as we can learn from Refs. [39–42,67,68] experiments on electron scattering off unstable nuclei will soon be possible. The application of a self-confining RI ion target will further make the luminosity for electron-scattering experiments high enough for measurements of cross sections to a sufficiently high momentum transfer to determine the shape of the charge distributions for the unstable nuclei. Numerical simulations have been made on ^{132}Sn [67,68]. According to the simulation parameters, the energy of the incident electrons is 500 MeV [67] and the scattering angle intervals are $\Delta\theta = 2.0^\circ$ [67]. This incident energy will extend the momentum transfer up to about $3.0\ \mathrm{fm}^{-1}$ for scattering angles of $30^\circ - 80^\circ$ [67]. This covers the range of moderate momentum transfer that has been considered in this paper. The small scattering angle intervals will also make the intervals of momentum transfer less than $0.09\ \mathrm{fm}^{-1}$. These show that future experiments will have a sufficiently high precision in measuring the cross sections of electron scattering on unstable nuclei. Therefore we consider that there are possibilities for the results given in this paper to be observed in the future experiments.

III. SUMMARY

In summary, we have calculated the charge density distributions, charge form factors, and differential cross sections for $N = 82$ and $N = 126$ isotonic nuclei. The variations of the charge distributions and charge form factors with proton number were investigated. It was found that the charge form factors and cross sections both near the minimums and near the maximums are sensitive to the increase of the proton number. When a new shell is occupied by protons, the charge form factors show a significant inward and upward shift for the isotonic chains considered. The isotonic shift of the charge form factors could be used to study the behaviors of wave functions of the outermost protons. Therefore it may also be useful for the exploration of the proton-halo phenomenon for light proton-rich nuclei for which the proton-halo means that the probability distributions of the outermost protons of some exotic proton-rich nuclei have an abnormally large rms radius (see Refs. [23,24] and Refs. [13,15,58]). Also, the results obtained in the present paper can be used as references for the future electron–RI beam experiments and tests of the reliability of the RMF model for the unstable nuclei.

Finally, we briefly discuss the expected difference between a neutron halo and a proton halo that is due to the instability of the system caused by an increase of the Coulomb force. It is well known that there exists only a strong interaction for the halo neutron in weakly bound neutron-rich nuclei. When the nuclei are close to the neutron drip line, the last one or two neutrons form a neutron halo when they occupy the orbit with low angular momentum and the binding energy at the orbit is very low. There is no Coulomb force between halo neutrons and the core because the charge number of neutrons is zero. Up to now neutron halos have been observed for nuclei such as ^{6,8}He, ^{11}Li, ^{11,14}Be, ^{17}B, and ^{19}C. Neutron halos have been well studied and will be further investigated in big laboratories [1–3,6,17,69]. However, studies on proton halos and proton skins of light proton-rich nuclei are rare compared with those on neutron halos. This means that there are many new phenomena on proton halos that will be explored by both experimental physicists and theoretical physicists. At the moment, studies on proton halos are exploratory, and the existence of proton halos in some light proton-rich nuclei has been established by independent experiments in some big laboratories. For example, both the RMF model and the shell model predict that there are proton halos in the ground state of $^{26-27}$P and ^{27,28}S [23,24,58]. The experiment from Michigan State University clearly shows that there are proton halos in $^{26-27}$P by the measurement of momentum distributions [13]. The measurement of the reaction cross sections [15] also shows that there is a proton halo in ^{27}P. Another independent measurement of the reaction cross section [70] confirms again that there is a proton halo in ^{27}P. Because the proton halo is a charged halo, it will provide a new opportunity and a new challenge for future studies. In particular, the role of the Coulomb interaction on proton halos is to be explored. We expect that the role of the Coulomb interaction will be dual. On the one hand, the Coulomb interaction is a repulsive potential and a barrier exists for a halo proton because of the common influence of an attracting strong interaction and the repulsive Coulomb interaction. It seems that the size of proton halo may be confined by the barrier. Actually, the situation is much complicated. Because the Coulomb interaction is a long-range one, the barrier can lie in a position near 6 fm for light nuclei and the rms radius of the halo proton can be anomalously larger than that of the core [58]. In this case the halo proton is in a weakly bound state such as $2S_{1/2}$ [23,24,58]. On the other hand, the existence of the repulsive barrier for a proton will lead to the appearance of new quasi-stationary states near the proton drip line because the Coulomb interaction is a long-range potential. The new quasi-stationary states belong to the special phenomenon of the proton-rich side, and this does not exist for the neutron-rich side. It is well known that there are proton emitters for proton-rich medium and heavy nuclei. The emitters can survive with a lifetime from 10^{-6} s to 10 s, although the decay energy of the last proton is positive. This lifetime is long enough for investigating the nuclear properties by radioactive beams. The last proton in this case stays in a quasi-stationary state because its single-particle energy is positive and its value is significantly lower than the height of the barrier (for a bound state the single-particle energy is negative in the RMF model or in the shell model). Although the single-particle energy is positive, the proton can stay in the nucleus for a long time because the width of the level is very narrow (a quasi-stationary state). These will bring new opportunities for investigating the proton halo by a future collider of the electron and unstable nuclei. As these problems are still open problems, we do not pursue them further. We believe that the field of the proton-rich side will be a living field to be explored and future facilities at RIKEN and at GSI can be used for this purpose. Perhaps the electron accelerator at CEBAF can also be used for these types of research [71].

ACKNOWLEDGMENTS

Z. Ren thanks W. Q. Shen, H. Q. Zhang, and Z. Y. Ma for discussions on electron scattering. This work is supported by the National Natural Science Foundation of China (grant no. 10535010 and grant no. 10125521), by the 973 National Major State Basic Research and Development of China (grant no. G2000077400), by the CAS Knowledge Innovation Project no. KJCX2-SW-N02, and by the Research Fund of Higher Education under contract no. 20010284036.

[1] I. Tanihata, Prog. Part. Nucl. Phys. **35**, 505 (1995).
[2] H. Geissel, G. Münzenberg, and K. Riisager, Annu. Rev. Nucl. Part. Sci. **45**, 163 (1995).
[3] A. Mueller, Prog. Part. Nucl. Phys. **46**, 359 (2001).
[4] I. Tanihata, H. Hamagaki, O. Hashimoto, Y. Shida, N. Yoshikawa, K. Sugimoto, O. Yamakawa, T. Kobayashi, and N. Takahashi, Phys. Rev. Lett. **55**, 2676 (1985).
[5] I. Tanihata, T. Kobayashi, O. Yamakawa, S. Shimoura, K. Ekuni, K. Sugimoto, N. Takahashi, and T. Shimoda, Phys. Lett. **B206**, 592 (1988).
[6] W. Mittig, J. M. Chouvel, Zhan Wen Long, L. Bianchi, A. Cunsolo, B. Fernandez, A. Foti, J. Gastebois, A. Gillibert, C. Gregoire, Y. Schutz, and C. Stephan, Phys. Rev. Lett. **59**, 1889 (1987).
[7] T. Kobayashi, O. Yamakawa, K. Omata, K. Sugimoto, T. Shimoda, N. Takahashi, and I. Tanihata, Phys. Rev. Lett. **60**, 2599 (1988).
[8] M. G. Saint-Laurent, R. Anne, D. Bazin, D. Guillemaud-Mueller, U. Jahnke, Jin Gen Ming, A. C. Mueller, J. F. Bruandet, F. Glasser, S. Kox, E. Liatard, Tsan Ung Chan, G. J. Costa,

C. Heitz, Y. El-Masri, F. Hanappe, R. Bimbot, E. Arnold, and R. Neugart, Z. Phys. A **332**, 457 (1989).
[9] T. Nilsson, F. Humbert, W. Schwab, H. Simon, M. H. Smedberg, M. Zinser, Th. Blaich, M. J. G. Borge, L. V. Chulkov, Th. W. Elze, H. Emling, H. Geissel, K. Grimm, D. Guillemaud-Mueller, P. G. Hansen, R. Holzmann, H. Irnich, B. Jonson, J. G. Keller, H. Klingler, A. A. Korsheninnikov, J. V. Kratz, R. Kulessa, D. Lambrecht, Y. Leifels, A. Magel, M. Mohar, A. C. Mueller, G. Münzenberg, F. Nickel, G. Nyman, A. Richter, K. Riisager, C. Scheidengerger, G. Schrieder, B. M. Sherrill, K. Stelzer, J. Stroth, O. Tengblad, W. Trautmann, E. Wajda, M. V. Zhukov, and E. Zude, Nucl. Phys. **A598**, 418 (1996).
[10] M. Zinser, F. Humbert, T. Nilsson, W. Schwab, Th. Blaich, M. J. G. Borge, L. V. Chulkov, H. Eickhoff, Th. W. Elze, H. Emling, B. Franzke, H. Freiesleben, H. Geissel, K. Grimm, D. Guillemaud-Mueller, P. G. Hansen, R. Holzmann, H. Irnich, B. Jonson, J. G. Keller, O. Klepper, H. Klingler, J. V. Kratz, R. Kulessa, D. Lambrecht, Y. Leifels, A. Magel, M. Mohar, A. C. Mueller, G. Münzenberg, F. Nickel, G. Nyman, A. Richter, K. Riisager, C. Scheidengerger, G. Schrieder, B. M. Sherrill, H. Simon, K. Stelzer, J. Stroth, O. Tengblad, W. Trautmann, E. Wajda, and E. Zude, Phys. Rev. Lett. **75**, 1719 (1995).
[11] N. A. Orr, N. Anantaraman, Sam M. Austin, C. A. Bertulani, K. Hanold, J. H. Kelley, D. J. Morrissey, B. M. Sherrill, G. A. Souliotis, M. Thoennessen, J. S. Winfield, and J. A. Winger, Phys. Rev. Lett. **69**, 2050 (1992).
[12] R. Anne, S. E. Arnell, R. Bimbot, H. Emling, D. Guillemaud-Mueller, P. G. Hansen, L. Johannsen, B. Jonson, M. Lewitowicz, S. Mattsson, A. C. Mueller, R. Neugart, G. Nyman, F. Pougheon, A. Richter, K. Riisager, M. G. Saint-Laurent, G. Schrieder, O. Sorlin, and K. Wilhelmsen, Phys. Lett. **B250**, 19 (1990).
[13] A. Navin, D. Bazin, B. A. Brown, B. Davids, G. Gervais, T. Glasmacher, K. Govaert, P. G. Hansen, M. Hellström, R. W. Ibbotson, V. Maddalena, B. Pritychenko, H. Scheit, B. M. Sherrill, M. Steiner, J. A. Tostevin, and J. Yurkon, Phys. Rev. Lett. **81**, 5089 (1998).
[14] R. Morlock, R. Kunz, A. Mayer, M. Jaeger, A. Muller, J. W. Hammer, P. Mohr, H. Oberhummer, G. Staudt, and V. Kolle, Phys. Rev. Lett. **79**, 3837 (1997).
[15] H. Y. Zhang, W. Q. Shen, Z. Z. Ren, Y. G. Ma, W. Z. Jiang, Z. Y. Zhu, X. Z. Cai, D. Q. Fang, C. Zhong, L. P. Yu, Y. B. Wei, W. L. Zhu, Z. Y. Guo, G. Q. Xiao, J. S. Wang, J. C. Wang, Q. J. Wang, J. X. Li, M. Wang, and Z. Q. Chen, Nucl. Phys. **A707**, 303 (2002).
[16] Z. Li, W. Liu, X. Bai, Y. Wang, G. Lian, Z. Li, and S. Zeng, Phys. Lett. **B527**, 50 (2002).
[17] Zhongzhou Ren and Gongou Xu, Phys. Lett. **B252**, 311 (1990).
[18] G. F. Bertsch and H. Esbensen, Ann. Phys. (NY) **209**, 327 (1991).
[19] M. V. Zhukov, B. V. Danilin, D. V. Fedorov, J. M. Bang, I. J. Thompson, and J. S. Vaagen, Phys. Rep. **231**, 151 (1993).
[20] P. G. Hansen, A. S. Jensen, and B. Jonson, Annu. Rev. Nucl. Part. Sci. **45**, 591 (1995).
[21] J. S. Al-Khalili, J. A. Tostevin, and I. J. Thompson, Phys. Rev. C **54**, 1843 (1996).
[22] T. Otsuka, N. Fukunishi, and H. Sagawa, Phys. Rev. Lett. **70**, 1385 (1993).
[23] Zhongzhou Ren, Baoqiu Chen, Zhongyu Ma, and Gongou Xu, Phys. Rev. C **53**, R572 (1996).
[24] B. A. Brown and P. G. Hansen, Phys. Lett. **B381**, 391 (1996).
[25] M. V. Zhukov and I. J. Thompson, Phys. Rev. C **52**, 3505 (1995).
[26] H. Iwasaki, T. Motobayashi, H. Akiyoshi, Y. Ando, N. Fukuda, H. Fujiwara, Zs. Fülöp, K. I. Hahn, Y. Higurashi, M. Hirai, I. Hisanaga, N. Iwasa, T. Kijima, T. Minemura, T. Nakamura, M. Notani, S. Ozawa, H. Sakurai, S. Shimoura, S. Takeuchi, T. Teranishi, Y. Yanagisawa, and M. Ishihara, Phys. Lett. **B481**, 7 (2000).
[27] T. Motobayashi, Y. Ikeda, Y. Ando, K. Ieki, M. Inoue, N. Iwasa, T. Kikuchi, M. Kurokawa, S. Moriya, S. Ogawa, H. Murakami, S. Shimoura, Y. Yanagisawa, T. Nakamura, Y. Watanabe, M. Ishihara, T. Teranishi, H. Okuno, and R. F. Casten, Phys. Lett. **B346**, 9 (1995).
[28] A. Ozawa, T. Kobayashi, T. Suzuki, K. Yoshida, and I. Tanihata, Phys. Rev. Lett. **84**, 5493 (2000).
[29] M. Stanoiu, F. Azaiez, Z. Dombrádi, O. Sorlin, B. A. Brown, M. Belleguic, D. Sohler, M. G. Saint Laurent, J. Lopez-Jimenez, Y. E. Penionzhkevich, G. Sletten, N. L. Achouri, J. C. Anglique, F. Becker, C. Borcea, C. Bourgeois, A. Bracco, J. M. Daugas, Z. Dlouhý, C. Donzaud, J. Duprat, Z. Fülöp, D. Guillemaud-Mueller, S. Grévy, F. Ibrahim, A. Kerek, A. Krasznahorkay, M. Lewitowicz, S. Leenhardt, S. Lukyanov, P. Mayet, S. Mandal, H. van der Marel, W. Mittig, J. Mrázek, F. Negoita, F. De Oliveira-Santos, Z. Podolyák, F. Pougheon, M. G. Porquet, P. Roussel-Chomaz, H. Savajols, Y. Sobolev, C. Stodel, J. Timár, and A. Yamamoto, Phys. Rev. C **69**, 034312 (2004).
[30] Z. H. Liu, X. Z. Zhang, and H. Q. Zhang, Phys. Rev. C **68**, 024305 (2003).
[31] Z. Y. Zhu, W. Q. Shen, Y. H. Cai, Y. G. Ma, Phys. Lett. **B328**, 1 (1994).
[32] Y. L. Ye, D. Y. Pang, D. X. Jiang, T. Zheng, Q. J. Wang, Z. H. Li, X. Q. Li, Y. C. Ge, C. Wu, G. L. Zhang, Q. Y. Hu, J. Wang, Z. Q. Chen, A. Ozawa, Y. Yamaguchi, R. Kanungo, and I. Tanihata, Phys. Rev. C **71**, 014604 (2005).
[33] R. Hofstadter, Rev. Mod. Phys. **28**, 214 (1956).
[34] T. W. Donnelly and J. D. Walecka, Annu. Rev. Nucl. Part. Sci. **25**, 329 (1975).
[35] T. W. Donnelly and I. Sick, Rev. Mod. Phys. **56**, 461 (1984).
[36] E. Moya de Guerra, Phys. Rep. **138**, 293 (1986).
[37] I. Sick, Prog. Part. Nucl. Phys. **47**, 245 (2001).
[38] H. De Vries, C. W. De Jager, and C. De Vries, At. Data Nucl. Data Tables **39**, 281 (1988).
[39] T. Suda, K. Maruyama, and I. Tanihata, RIKEN Accel. Prog. Rep. **34**, 49 (2001).
[40] T. Suda, in *Proceedings of the International Workshop XXXII on Gross Properties of Nuclei and Nuclear Excitations*, edited by M. Buballa, J. Knoll, W. Nörenberg, B.-J. Schaefer, and J. Wambach (GSI, Darmstadt, 2004), p. 235.
[41] An International Accelerator Facility for Beams of Ions and Antiprotons, GSI report, 2002.
[42] H. Simon, in *Proceedings of the International Workshop XXXII on Gross Properties of Nuclei and Nuclear Excitations*, edited by M. Buballa, J. Knoll, W. Nörenberg, B.-J. Schaefer, J. Wambach (GSI, Darmstadt, 2004), p. 290.
[43] E. Moya de Guerra, E. Garrido, and P. Sarriguren, in *Proceedings of the Seventh International Spring Seminar on Nuclear Physics*, edited by A. Covello (World Scientific, Singapore, 2002), p. 63.
[44] A. N. Antonov, M. K. Gaidarov, D. N. Kadrev, P. E. Hodgson, and E. Moya de Guerra, Int. J. Mod. Phys. E **13**, 759 (2004).
[45] A. N. Antonov, D. N. Kadrev, M. K. Gaidarov, E. Moya de Guerra, P. Sarriguren, J. M. Udias, V. K. Lukyanov, E. V. Zemlyanaya, and G. Z. Krumova, Phys. Rev. C **72**, 044307 (2005).

[46] Z. Wang and Z. Ren, Phys. Rev. C **70**, 034303 (2004).
[47] Z. Wang and Z. Ren, Phys. Rev. C **71**, 054323 (2005).
[48] J. Cavedon, J. B. Bellicard, B. Frois, D. Goutte, M. Huet, P. Leconte, X.-H. Phan, S. K. Platchkov, and I. Sick, Phys. Lett. **B118**, 311 (1982).
[49] J. R. Ficenec, L. A. Fajardo, W. P. Trower, and I. Sick, Phys. Lett. **B42**, 213 (1972).
[50] J. Heisenberg, R. Hofstadter, J. S. McCarthy, I. Sick, B. C. Clark, R. Herman, and D. G. Rarenhall, Phys. Rev. Lett. **23**, 1402 (1969).
[51] A. Baker, Phys. Rev. **134**, B240 (1964).
[52] J. D. Walecka, Ann. Phys. (NY) **83**, 491 (1974).
[53] J. D. Walecka, Phys. Lett. **B94**, 293 (1980).
[54] B. D. Serot and J. D. Walecka, Adv. Nucl. Phys. **16**, 1 (1986).
[55] Y. K. Gambhir, P. Ring, and A. Thimet, Ann. Phys. (NY) **198**, 132 (1990).
[56] C. J. Horowitz and B. D. Serot, Nucl. Phys. **A368**, 503 (1981).
[57] Z. Ma, H. Shi, and B. Chen, Phys. Rev. C **50**, 3170 (1994).
[58] Z. Ren, W. Mittig, and F. Sarazin, Nucl. Phys. **A652**, 250 (1999).
[59] Z. Ren, W. Mittig, B. Chen, and Z. Ma, Phys. Rev. C **52**, R20 (1995).
[60] Y. Sugahara and H. Toki, Nucl. Phys. **A579**, 557 (1994).
[61] W. Z. Jiang and Y. L. Zhao, Phys. Lett. **B617**, 33 (2005).
[62] B. G. Todd-Rutel and J. Piekarewicz, Phys. Rev. Lett. **95**, 122501 (2005).
[63] W. Greiner and J. Reinhardt, *Quantum Electrodynamics* (Springer-Verlag, Berlin, Heidelberg, 1992).
[64] G. Audi, A. H. Wapstra, and C. Thibault, Nucl. Phys. **A729**, 337 (2003).
[65] G. C. Li, M. R. Yearian, and I. Sick, Phys. Rev. C **9**, 1861 (1974).
[66] I. Sick and J. S. McCarthy, Nucl. Phys. **A150**, 631 (1970).
[67] T. Suda, M. Wakasugi, Prog. Part. Nucl. Phys. **55**, 417 (2005).
[68] M. Wakasugia, T. Sudab, and Y. Yano, Nucl. Instrum. Methods A **532**, 216 (2004).
[69] H. Sakurai *et al.*, Phys. Lett. **B448**, 180 (1999).
[70] Z. H. Liu *et al.*, Phys. Rev. C **69**, 034326 (2004).
[71] J. D. Walecka, *Theoretical Nuclear Physics and Subnuclear Physics* (Oxford University Press, Oxford, 1995).